Properties of Fractal Divinylbenzene Microgels

Markus Antonietti* and Christine Rosenauer

Institut für Physikalische Chemie der Universität Mainz, Jakob Welder Weg 15, D-6500 Mainz, West Germany

Received August 31, 1990; Revised Manuscript Received January 21, 1991

ABSTRACT: Microgels, small cross-linked structures with molecular weights of 10^5 g/mol $\leq M_w \leq 10^8$ g/mol, have been synthesized via radical copolymerization of styrene and 10 mol% technical divinylbenzene in an inert solvent. The resulting products have been fractionated and characterized with GPC, viscometry, static and dynamic light scattering, small-angle neutron scattering, and dynamic mechanical shear experiments. These systems, when synthesized slightly below the critical transition from micro- to macrogelation, exhibit a scalable behavior of their static and dynamic properties and can be described as fractal structures. The data show that it is possible to generalize the gel transition to include all effects of dilution.

I. Introduction

The synthesis of microgels made of styrene and divinylbenzene has been described by Staudinger and Husemann in 1935.[1] They made the observation that reaction mixtures consisting of less than 8% divinylbenzene in an inert diluent do not form macroscopic gels but form soluble products with a low intrinsic viscosity. The molecular weights that they studied were in the range M_n = 20000–40000 g/mol, and their attempts to synthesize larger molecules failed. Since their discovery relatively few studies concerning the structural and dynamical behavior of these or similar microgels can be found in the literature.

On the other hand, technical interest in microgels has increased in recent years because binders and coatings containing defined microgels exhibit improved properties.[2,3] Also, applications as drug or enzyme carriers have been discussed.[4] Since microgels also present a potential access to polymer systems with new structural ordering,[5,6] we wish to deepen the understanding of the relationship between synthetic conditions and the resulting product properties.

In previous publications[7,8] we have shown that the observations of Staudinger and Husemann can be generalized to all cross-linking reactions. Increasing the amount of solvent present during cross-linking also increases the probability of internal cyclization until the macroscopic nature of cross-linking breaks apart. The regimes of micro- and macrogelation are separated by a sharply defined critical volume fraction of polymer that can be described in analogy with the gel transition of classical gelation theory. Closely below this volume fraction, structures with molecular weights of 10^6 g/mol $< M_w < 10^9$ g/mol can be easily obtained.[17] In addition, these molecules exhibit properties that can be described by using the theory of "fractal" structures.

The critical polymer concentration depends on cross-link density and the geometrical parameters of the molecules. Even pure cross-linking agents can be polymerized, still resulting in microgels. A skillful experiment supporting this statement is given by the cross-linking polymerization of norbornadiene via metathesis.[9] Due to the reversibility of this reaction, the critical concentration can even be "titrated" and was determined to 0.2 mol/L or a 2% volume fraction. It should be mentioned that the authors of ref 9 have interpreted this phenomenon in a slightly different way.

The scope of the present work is a repetition of the old Staudinger/Husemann experiments followed by a characterization of the products with modern techniques of polymer analysis, e.g., GPC, viscometry, static and dynamic light scattering, small-angle neutron scattering, and dynamic mechanical experiments.

Through these experiments, we wish to gain more information about the structure and dynamics of these microgels. We also describe some unconventional properties of such molecules.

II. Experimental Section

II.1. Polymer Synthesis. The microgels are synthesized by simple radical copolymerization in benzene solution. We decided to synthesize the microgels using monomer mixtures of styrene and technical divinylbenzene (DVB, 50% was a mixture of divinylbenzene isomers, the remainder mainly ethylstyrene) since these systems are more easily handled than pure DVB microgels. Furthermore, the dynamic mechanical measurements in the melt can be performed only with the copolymers. During the experiments it become apparent that systems with 5–20% technical DVB copolymerized with styrene exhibit most of the characteristics of the pure DVB microgels but offered a much lower glass transition and a better solubility. It was also found that the use of pure *p*-divinylbenzene instead of technical DVB does not significantly change the product properties.

However, as a result of the copolymerization of the DVB with styrene and ethylstyrene, the critical weight fraction of the micro-/macrogelation transition for this monomer mixture is shifted toward higher values when the amount of DVB is decreased. Compared to the Staudinger value of 0.08 for pure DVB, we determine a value of 0.102 for a system with 10% DVB and 0.120 for systems with 5% DVB (percentage in relation to the complete amount of monomer).

Since the applied synthetic procedure is a standard technique, it is just briefly delineated on the basis of one typical reaction mixture. DVB, styrene, and benzene are dried over $LiAlH_4$ and freshly distilled prior to use. DVB, 5.67 g, styrene, 45.33 g, and benzene, 449.0 g, are mixed and degassed and 250 mg of azobis(isobutyronitrile) (AIBN) is added. The reaction mixture is stirred for 20 days at 70 °C, and 100-mg portions of AIBN are added three times. After that, the extent of reaction in regard to the mass of polymer is found to be larger than $p > 0.96$.

In a second step, the remaining double bonds are reacted with silane derivatives to prevent further cross-linking of the isolated product. To the described product, 5 mL of dimethylphenylsilane and 0.5 mL of H_2PtCl_6 solution (3%) are added, and the mixture is stirred for 2 days at room temperature. After this treatment, the polymer material can be isolated and processed without influencing the original molecular weight distribution, as tested by GPC after most steps of the subsequent sample treatments. Therefore, these DVB microgels can be regarded as chemically stable, in contrast to spherical microgels with pendant vinyl groups.[2,5]

A portion of this initially very polydisperse microgel product is fractionated three times with methanol/THF mixtures, thus

0024-9297/91/2224-3434$02.50/0

resulting in typically 5–10 fractions with a moderate polydispersity.

II.2. Solution Viscosity Measurements. The solution viscosity measurements are performed in toluene at 20.0 °C with an automatic Schott AVS300 instrument (Ubbelohde viscosimeter), which allows the determination of flow times with an accuracy of 0.01 s. The solutions are made by dissolving the samples in freshly distilled, sodium-dried toluene. The flow times are determined for six to nine concentrations ranging from 20 to 1 g/L.

II.3. Static and Dynamic Light Scattering. Light scattering experiments were carried out for seven fractions in toluene at 20.0 °C. The spectrometer and procedure for simultaneous static and dynamic light scattering are extensively described in previous publications.[10,11] The measurements are performed at the 647.1-nm line of a krypton ion laser (Spectra-Physics 2025). We adopt for the refractive index increment the value for linear polystyrene in toluene, $\partial n/\partial c = 0.110$ ($T = 20$ °C). The final concentrations range between 10^0 and 10^{-2} g/L and are realized by filtering a more concentrated solution through Millipore 0.45-μm PTFE filters into the cuvette and subsequent dilution within the optical cell with a controlled amount of filtered solvent. Using this method, the most accurate and reproducible concentrations are obtained. On the other hand, filtering a very dilute solution causes a significant loss of concentration due to the filter as proved by a RI detector. The molecular masses of the samples are determined by extrapolating data from four different concentrations covering a factor of 4.

II.4. Small-Angle Neutron Scattering. The small-angle neutron scattering experiments (SANS) are carried out at the Institut Laue-Langevin in Grenoble, France, using the small-angle diffractometer D11.[12] The measurements on D11 are performed by using sample-to-detector distances of 2, 5, 10, and 20 m and an incident neutron wavelength of $\lambda = 0.6$ nm. The distribution of wavelengths $\Delta\lambda/\lambda$ is 10%. The neutron counts on the two-dimensional detector are radially averaged, normalized to the incoming neutron dose, and corrected for transmission and sample volume. The incoherent scattering of water is taken as a calibration for absolute scattering intensity and to correct inhomogeneities of the detector.

The experiments are carried out in optical cuvettes (boron-poor Suprasil from Hellma Co.) with path lengths of 1 and 2 mm. Protonated micronetworks in deuterated toluene (99.5% d, Aldrich Co.) are prepared in a 1% solution as mentioned above. During the measurements the temperature is held at $T = 20.0$ °C.

All measurements are corrected for the scattering of the solvent by subtraction of the independently measured values of the cuvettes filled with pure toluene.

II.5. DSC Measurements. DSC measurements are performed with a Perkin-Elmer Model DSC 2 C instrument. Pellets of 10–20 mg are heated in aluminium pans with a heating or cooling rate of 10 K/min giving a small hysteresis. The samples are measured two to four times. The first run was used for equilibration only.

II.6. Dynamic Mechanical Experiments. The micronetwork samples are precipitated from solution and carefully dried overnight in vacuo at 80 °C. By compression molding at 150 °C, optically clear disks with a diameter of 13 mm are prepared, fitting the geometry of a plate/plate rheometer. This treatment does not influence the original molecular weight distribution, as checked by GPC.

A Rheometrics RMS 800 apparatus is used in an oscillating low-amplitude mode in a frequency range between 10^{-2} and 10^2 rad/s^{-1} with an amplitude of 2%. It is checked that our measurements are within the linear regime, which typically goes up to 30% strain. The measurements are controlled by a FRT2000 frequency response analyzer, which also records the complex torque. A stream of dry nitrogen is blown over the sample in order to avoid thermal oxidative damage during the measurements performed at 130–190 °C. After heating the sample to the maximum temperature, the measurements at 150 °C is repeated in order to check for alteration. During these measurements, it turns out that DVB microgels are relatively stable up to 170 °C, whereas a temperature of 190 °C should only be applied for a few minutes. In some cases, an irreversible change of the spectra is caused by neglecting these limitations. The presented master curve considers only data obtained in the stable region.

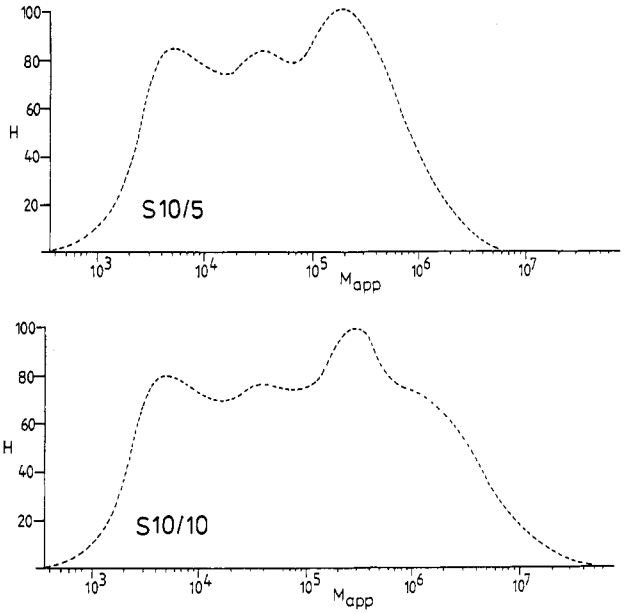

Figure 1. GPC spectra of the unfractionated samples S10/5 (a, top) and S10/10 (b, bottom). The relative amount H (by weight) is plotted versus the apparent molecular weight M_{app}, as obtained by calibration with linear polystyrene.

III. Results and Discussion

III.1. Synthesis and Characterization with GPC. Microgels with 5–20% DVB (the remainder styrene) exhibit most of the typical microgel properties but offer the advantage of a much lower glass transition temperature and a better solubility.

For those reasons, the structural and dynamic behavior of microgels will be exemplarily discussed by the sample containing 10% DVB. However, it has been checked that most of the properties can be generalized to all systems with DVB contents between 5% and 50%.

The initial products, as isolated from the reaction mixture, are very polydisperse. Parts a and b of Figure 1 present the GPC spectra of the samples S10/5 and S10/10, corresponding to cross-linking reactions performed at monomer contents of $\Phi_P = 0.05$ and $\Phi_P = 0.10$, respectively. The latter value is just slightly below the critical volume fraction where macroscopic gelation occurs. The samples are named by "S" (Staudinger microgels) and two numbers. The first denotes the inversed cross-linking density the second the percentage of monomer present during the cross-linking. Molecular weights M_{app} are apparent values since the GPC was calibrated with linear polystyrene samples. The relation of M_{app} to the real molecular weight will be discussd later.

In both cases, the number-average molecular weight M_n is low. The apparent values of M_n(app) ≈ 10 200 or 11 800 g/mol are below the reported values of 20 000 to 40 000 g/mol of the Staudinger experiments,[1] which is possibly due to the relative nature of our data. In contrast to that, the weight-average M_w and the polydispersity index M_w/M_n are very large and seem to diverge by approaching the transition from micro- to macrogelation.

A similar critical behavior is known for the "classical" gel transition (see, for instance, refs 3, 14, 15, and 16), although pronounced differences in the experimental scenario exist. Classically, the number of structural cross-links is controlled by the extent of reaction, whereas in

Table I
Characterization of Microgel Fractions of the Series S10/10 with GPC[a]

sample	M_n(app)	M_w(app)	M_w/M_n
S10/10	(11.8×10^3)	(2.67×10^5)	(22.6)
S10/10F1	(4.73×10^5)		
S10/10F2	(5.46×10^5)		
S10/10F3	3.59×10^5	7.18×10^5	2.00
S10/10F4	3.42×10^5	6.93×10^5	2.02
S10/10F5	2.52×10^5	5.34×10^5	2.12
S10/10F6	1.42×10^5	2.55×10^5	1.80
S10/10F7	5.80×10^4	1.30×10^5	2.56
S10/10F8	2.97×10^4	9.04×10^4	3.04
S10/10F9	2.19×10^4	5.44×10^4	2.50
S10/10F10	4.39×10^3	1.23×10^4	2.80

[a] Due to the calibration with linear polystyrene, only apparent values can be shown. The values in parentheses are disturbed by the excluded volume of the GPC combination used.

the present case only the cross-linking topology throughout dilution has been changed (e.g., the number of cross-links incorporated in small cycles). It is not obvious that both variations result in the same structures and the same critical behavior.

Using the Flory–Stockmayer theory for gelation,[13-15] we can calculate an apparent molecular weight Λ_n of the "primary" chain, which can be interpreted as the average structure formed between initiation and termination of the polymerization process caused by one propagating radical. We obtain a value of about $\Lambda_n \approx 8000$ g/mol. In other words: polymerization of such a microgel proceeds by addition of about 75 monomer units to the free radical before termination occurs. This value is very low compared to values known for the radical polymerization of linear polystyrene.

Assuming the validity of the Flory–Stockmayer theory for the position of the gel point, we can calculate the amount of pendent double bonds incorporated in the same primary chain (cross-linking molecules involved twice in the same kinetic process), which are inefficient for intercatenar cross-linking. Considering the many approximations performed (as the relative nature of the GPC data), we can estimate roughly a value of about 95%. This is in good agreement with results of Burchard and Schmidt[17] who determined a value of 94% for the anionic copolymerization of styrene and divinylbenzene in a 5% solution. Therefore, dilution changes the cross-linking topology in such a way that at least most of the cross-links are involved in small cyclic substructures. Only a small number of molecules act as cross-links in the classical sense and are seen in a macrogelation process. This observation has been qualitatively made for many cross-linking copolymerization reactions performed in dilution and also exists in the early stages of bulk polymerization[18-20] (we call the attention of the interested reader to a review of Dusek[21]).

We have not corrected the cross-linking efficiency for the substantial number of unreacted double bonds, the consideration of which would increase the apparent efficiency. Titration experiments performed with nonprotected microgels as proposed by Seitz[22] indicate an amount of unreacted pendent vinyl groups below 10%.

For further examinations, the microgels have to be fractionated thus resulting in microgel fractions with a moderate polydispersity. In addition, this procedure allows the observation of molecular weight dependencies by comparing the results of the different fractions. In the present case of sample S10/10, the separation was performed by a 3-fold fractionation from THF solutions with methanol as a nonsolvent. The GPC characterization of the resulting 10 fractions is shown in Table I.

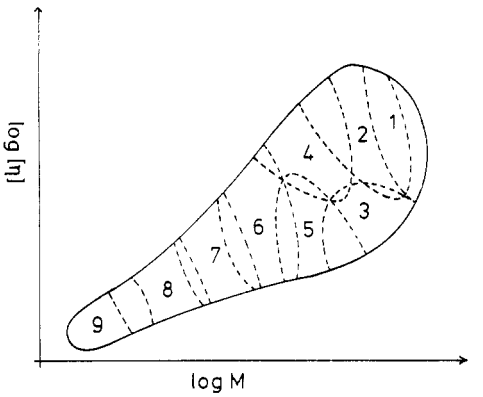

Figure 2. Schematic presentation of a possible two-dimensional product distribution and fictive positions of the fractions (numbered).

Table II
Data for Different Microgel Fractions in Toluene at 20.0 °C[a]

fraction	M_w/g mol^{-1}	r_G/ nm	r_H/ nm	$[\eta]$/cm^3 g^{-1}	r_η/ nm	r_G/r_H	r_η/r_H
S10/10F1	30×10^6	155	104.3	227	102.6	1.49	0.98
S10/10F2	18×10^6	128	85.2	210	84.3	1.50	0.99
S10/10F3	4.2×10^6	62	38.6	94.5	39.7	1.61	1.03
S10/10F4	3.1×10^6	52	33.2	90.2	35.4	1.57	1.07
S10/10F5	2.0×10^6	43	27.8	89.7	30.5	1.55	1.10
S10/10F6	5.1×10^5	25.5	14.8	51.5	16.1	1.72	1.09
S10/10F7	3.1×10^5	22.6	11.7	44.3	13.0	1.93	1.11

[a] $[\eta]$ intrinsic viscosity; M_w molecular mass determined with light scattering; r_G radius of gyration; r_H hydrodynamic radius determined by QELS; r_η viscosimetric radius calculated from $[\eta]$.

The apparent polydispersities are between $1.8 \leq M \leq 3.0$, which can be accepted for the discussion of the data.

During the fractionation it also turned out that the samples possess a worse solubility in THF than linear polystyrene; the precipitation occurs at much lower amounts of methanol. In good agreement, commonly known Θ-solvents for polystyrene are nonsolvents for the examined microgels in the complete accessible temperature range.

For further discussion one should keep in mind that fractionation is not a simple action in complex systems as cross-linked structures or copolymers. In addition to the usual primary polydispersity related to the distribution of molecular weights, a secondary polydispersity exists in these systems that describes the distribution of hydrodynamic volume at a given molecular weight. A fractionation is sensitive to both parameters, and comparing the results of different fractions can be severely disturbed by a wrong separation of the samples. For illustration, Figure 2 sketches an extreme case of such a two-dimensional product distribution and possible localizations of the fractions. In this case, the molecular weight dependent intrinsic viscosity will not obey a scaling dependence, whereas some relationship may be obtained from the right averages.

III.2. Light Scattering and Viscometry in Solution. Table II summarizes the data from the fractions S10/10F1–S10/10F7 as obtained by viscometry and static and dynamic light scattering in toluene at 20.0 °C. The last three fractions (S10/10F8–S10/10F10) are too small to allow a precise determination of their properties.

If we relate the intrinsic viscosities to the molecular weights, M_w, we observe a stepwise behavior which clearly indicate that the origial reaction mixture is also fractionated in relation to the secondary polydispersity. In particular, the samples S10/10F3–S10/10F5 exhibit nearly

the same $[\eta]$ value but differ by a factor of 2 in their molecular weights.

We have also calculated the viscometric radius r_η according to eq 1 (taken from ref 23):

$$r_\eta = \left[\frac{3[\eta]M_w}{10\pi N_L}\right]^{1/3} \quad (1)$$

Due to the inclusion of the molecular weight, r_η has the advantage of being less influenced by the secondary polydispersity.

Figure 3 presents the molecular weight dependencies of the radius of gyration $r_G \equiv \langle s^2\rangle_z^{1/2}$, the hydrodynamic radius $r_H \equiv \langle r_h^{-1}\rangle_z^{-1}$ and the viscometric radius r_η in a double-logarithmic plot.

One observes that r_H and r_η are nearly equal. By fitting the data to scaling relationships, we obtain

$$r_\eta\,(M) = (3.81 \times 10^{-11})M_w^{0.46} \quad (2)$$

$$r_H\,(M) = (3.18 \times 10^{-11})M_w^{0.47} \quad (3)$$

$$r_\eta/r_H \approx 1.04 \quad (4)$$

The molecular weight dependence of r_G is poorly described by a power law. Excluding the two smallest values, we obtain

$$r_G\,(M) = (4.83 \times 10^{-11})M_w^{0.47} \quad (5)$$

$$r_G/r_H = 1.51 \quad (6)$$

Therefore, all exponents a are practically equal and range between the value of massive spheres ($a = 0.33$) and the unperturbed Gaussian chain ($a = 0.50$). This behavior is in good agreement to the expected shape for cross-linked polymers.

The ratio r_η/r_H slightly exceeds unity, a behavior known for randomly branched systems.[24] Within the data set, we can observe a systematic decrease from 1.1 to 1.0 with increasing molecular weight, thus indicating a decreasing influence of hydrodynamic draining. In addition, the experimentally determined value of $r_G/r_H \approx 1.5$ is equivalent to the value of linear chains in a good solvent ($r_G/r_H = 1.5$, see ref 25) and exceeds by more than a factor of 2 the values of systems with spherical symmetry.[26,27] We can also relate the behavior of DVB microgels to that one of linear polystyrene in a good solvent by calculating the contraction factors $g^{0.5} \equiv r_G(\mu\text{gel})/r_G(\text{lin})$ and $h \equiv r_H(\mu\text{gel})/r_H(\text{lin})$. Taking the corresponding relationships of r_G and r_H for linear chains from the literature,[10,25] we obtain

$$g^{0.5} = 4.35M^{-0.14} \quad (7)$$

$$h = 2.93M^{-0.11} \quad (8)$$

$$h/g^{0.5} = 0.67M^{0.03} \quad (9)$$

The molecular weight dependencies of $g^{0.5}$ and h parallel each other. In the relevant regime of molecular weights of our experiments, the ratio $h/g^{0.5}$ is very close to unity. DVB microgels with $M_w = 2 \times 10^6$ g/mol for instance possess characteristic radii that are 40% smaller than the corresponding ones of linear chains.

Using the universal calibration relationship,[28] we also find that this contraction agrees with the ratio of the apparent M_w determined by GPC and M_w determined by light scattering.

Extrapolating the contraction ratios toward molecular weights in the order of the primary chain length ($M_w \approx 3 \times 10^4$ g/mol), we obtain for this region practically no contraction at all. Structures and substructures on this length scale apparently behave as linar chains. This fact also gives good evidence for the validity of the M_n value of the unfractionated sample as taken from the GPC and the subsequent conclusions as presented above.

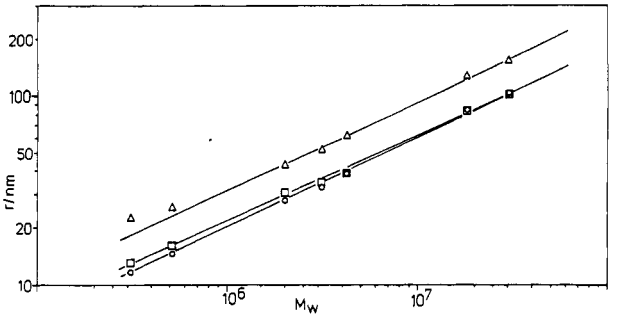

Figure 3. Radius of gyration r_G (△), viscometric radius r_η (□), and hydrodynamic radius r_H (○) of the fractions S10/10F1–S10/10F7 plotted versus the molecular weight as determined by light scattering. The straight lines present the scaling relationships as given in the text.

From all these data, we can visualize DVB microgels as quite open structures, more densely packed than linear chains, but evidently more transient than spheres or other compact particles.

In a second step, the data of DVB microgels are compared with analogous data obtained from other cross-linked structures.

On the one hand, the scaling relationships eqs 2, 3, and 5 and most of the combined structure properties are surprisingly similar to the corresponding equations determined for model micronetworks.[7] These systems are synthesized by a completely different chemical pathway but are also close to the transition from micro- to macrogelation. This fact must be emphasized since the cross-linking density of the present systems is a factor of 10 higher than the one of the model micronetworks. Nevertheless, we expect some differences on a very local scale where the influence of the different geometrical structure elements should be observable.

The radius of gyration of the DVB microgels exceeds by ~18% that of a model micronetwork with comparable molecular weight. This small difference is larger than the experimental error and is probably caused by slightly higher polydispersisties of the DVB microgel fractions.

On the other hand, it is interesting to compare the data with corresponding experiments performed with copolymers made of styrene and 1,4-divinyltetrachlorobenzene.[29] These systems have also been synthesized in the subcritical regime of cross-linking but with a higher monomer concentration ($\Phi_P \approx 0.5$) and a much lower cross-link density. Also these systems obey nearly the same molecular weight dependencies of r_G and r_η. Only the absolute values at a given molecular weight are slightly higher, which can be caused by the structural influence of long dangling ends. These structure elements appear in substantial number in systems with low cross-link densities.

The comparison between these three systems is of importance since all of them are synthesized just below the gel transition, but the reaction parameters, the cross-link density, and even the chemical pathway are totally different. From this we can deduce that the guidelines for the structure of such systems are mainly determined by the proximity to this phase transition and only to a lesser extent by the actual chemical composition.

III.3. Small-Angle Neutron Scattering in Solution. More information about the inner structure on the length scale of typical structure elements of the DVB microgels can be obtained by small-angle neutron scattering

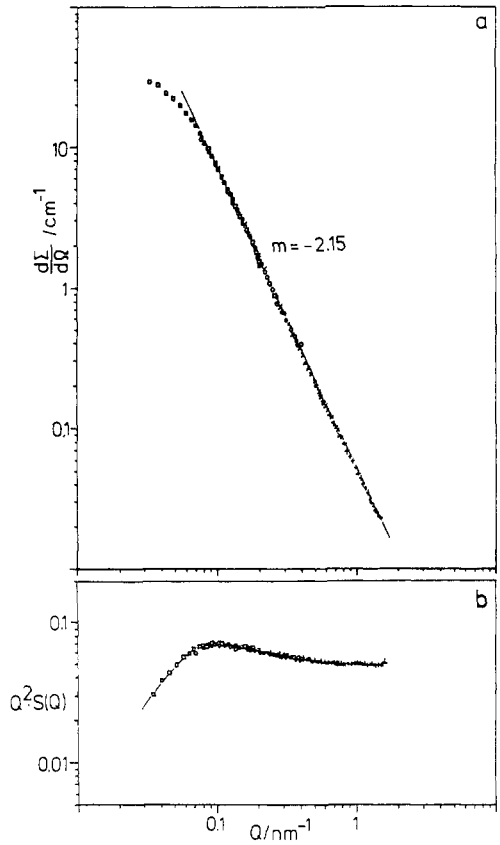

Figure 4. Master plot of the scattering behavior of sample S10/10F2 in a 1% toluene solution at 20.0 °C as obtained by superposition of SANS data of four different detector positions. Part a presents the data in a double-logarithmic plot, part b the same sets of data in a logarithmic Kratky plot. The straight line approximates the data with a scaling relationship with $d_f = 2.15$.

(SANS). Here, the spatial pair correlation function of monomer units is determined by measuring its Fourier transform, the dependence of the absolute scattering cross section $d\Sigma/d\Omega$ on the scattering vector Q (see, for instance, refs 30 and 31).

For noncompact bodies with radial density function obeying a scaling law, the relation between the density distribution and the angular dependence of the scattering intensity is very simple. We note the dependence of the molecular weight with the radius of gyration r_G:

$$M_w \sim r_G^{d_f} \tag{10}$$

Fourier transformation from r to Q space results in

$$(d\Sigma/d\Omega)(Q) \sim Q^{-d_f} \tag{11}$$

If relation 10 or 11 holds over several decades, it can be used to define the objects as fractals with the dimension d_f.[32,33]

Due to restrictions in beam time, we have only measured 1% solutions of DVB microgels in toluene. In respect to the values of the intrinsic viscosity, these measurements cannot properly be interpreted as dilute solution experiments since they are performed in proximity of c^*. Consequently, we cannot determine molecular parameters such as the molecular weight or radius of gyration from these measurements. However, in the region of higher momentum transfer corresponding to the inner architecture of these systems, the influence of concentration should be neglectible.

Figure 4 presents the master curve of the absolute scattering cross section $d\Sigma/d\Omega$ for sample S10/10F2, as obtained from the superposition of four different detector positions on D11 (2.5, 5, 10, and 20 m). The same set of data is plotted twice: Figure 4a shows the data in a double-logarithmic presentation whereas a logarithmic Kratky plot has been chosen for Figure 4b.

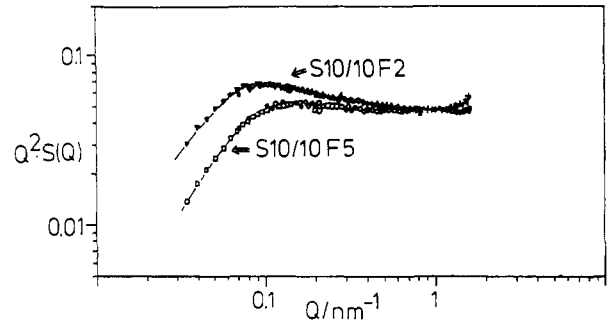

Figure 5. Comparison of the SANS curves of samples S10/10F2 and S0/10F5 (low-density fraction) in the logarithmic Kratky presentation.

As seen in Figure 4a, the data in the central regime of the scattering profile can be described by a scaling relationship. We obtain $d_f = 2.15 \pm 0.03$. The excellence of the description is better seen in the Kratky presentation where minor deviations become observable. Here, we state a slight bending of the curve toward higher Q values, where we observe a change toward the scattering behavior of the structure elements that are expected to behave similar to linear chains.

The validity of the power law at low Q values is limited by the overall molecular size of the DVB microgels. These two effects, caused by the chemical nature of DVB microgels, restrict a further extent of the fractal regime. From the present data, we can deduce only that the scaling is fulfilled on a length scale of 6 nm $\leq \xi \leq$ 60 nm.

However, using the relation between eqs 10 and 11, we can compare the results from light and neutron scattering. We can calculate from the dependence of the radius of gyration on the molecular weight (eq 5) a value for d_f(LS) $= 1/0.47 \approx 2.13 \pm 0.04$, which excellently agrees with d_f(NS) = 2.15. Due to this agreement, two major conclusions can be made:

DVB microgels synthesized close to the transition from micro- to macrogelation are self-similar. Small substructures of a large molecule behave in the same way as small molecules of the same kind.

The scaling relationship for d_f is not only fulfilled on the length scale of neutron scattering but can be extended to the scale of the typical radii of gyration, at least up to 150 nm.

These facts indicate that the description of these systems as fractals is valid.

Since we have observed a remarkable influence of fractionation on the inner density of the microgels (as indicated by the inverse of the intrinsic viscosity), we must examine the influence of the secondary polydispersity on the scaling of the pair correlation function. For that, we compare the neutron scattering curves of a "high density" fraction with a "low density" one.

Figure 5 presents the master curves of the absolute scattering cross section for the samples S10/10F2 and S10/10F5 in a logarithmic Kratky plot, which resolves minor differences. We have chosen these two fractions for comparison, since they exhibit experimentally the most pronounced differences within the examined sample set. Due to the lower absolute molecular weight, the scaling regime of sample S10/10F5 is less extended. A description of the center part of the scattering curve results in $d_f = 2.05 \pm 0.03$, a value significantly below the $d_f = 2.15$, as

determined above. All other fractions show a scattering profile that in the middle part is practically identical with that of S10/10F2.

From these results we have to conclude the fractionation can influence the determination of the fractal dimensionality, since we have separated the crude product not only with respect to molecular weight but also with respect to the inner density. In using the procedure, we have to take into account a systematic uncertainty, which can be estimated conservatively as twice the experimental error.

Considering this restriction, the value for d_f can be compared once more with experimental values of other groups and theoretical predictions. Chu et al. examined a critically branched epoxy polymer with synchroton radiation and determined a value of $d_f = 2.17 \pm 0.04$, in good agreement with the data presented here.[34] Adam et al. obtained for a fractionated sample close to its gel transition $d_f = 1.98$,[35] a value that significantly deviates from the first two experiments.

Model micronetworks behave slightly different. In a good solvent, they are swollen ($d_f = 1.9$) on a local scale, whereas the molecular weight dependence of r_G is similar to that of DVB microgels. In a Θ-solvent, the scaling exponent is given by $d_f \approx 2.5$. Unfortunately, we have found no Θ-solvent for DVB microgels. For this reason, a closer comparison must await further experiments.

Describing the gel transition with the percolation theory,[36] we obtain, for the fraction with the largest clusters, $d_f = 2.5$ in the unperturbed state or $d_f = 2.0$ in a good solvent.[37] These predictions are in good agreement with the results obtained for model micronetworks or with the Adam data. The present data and the results of Chu deviate significantly from this prediction.

In contrast to the more "static" nature of simple percolation, one can also describe the structure of microgels with dynamic aggregation models, which are also called "dynamic" percolation models. These models are very successfully used for description of inorganic colloidal aggregates.[33]

In regard to the chemical situation of DVB polymerization in dilute solution, it is appropriate to use the model of reaction-limited cluster/cluster aggregation (RLCA). Within this model, we theoretically obtain $d_f \approx 2.09$. This value agrees with the experimental observations presented above, especially when the experimental uncertainty due to the influence of the secondary polydispersity is concerned.

The use of dynamic aggregation models explains the difference between DVB microgels and model micronetworks in regard to the structure on a local scale. In contrast to the time-consuming synthesis of the radically polymerized DVB microgels, model micronetworks are made via a fast ionic addition of elementary chains, a scenario that can be better described by a diffusion-controlled monomer/cluster addition or the Witten–Sander model. Also this model results in a $d_f \approx 2.5$ for the unperturbed state. For good solvent conditions this value must be corrected for the influence of the excluded volume, in analogy to the theory of percolation clusters.[37]

III.4. Dynamic Mechanical Experiments. A power law of structural properties or connectivity should also be reflected in the dynamic behavior of these systems. In fact, the fractal nature of near-critical gels was first observed by means of the dynamics of those systems. In their pionerring work, Winter and co-worker found that the storage modulus G' parallels the loss modulus G'' and scales with the shear frequency ω as $G' \sim G'' \sim \omega^{0.5}$ within the whole accessible frequency range.[38-40]

Table III
Mechanical Shift Parameters log a_T for Different Polystyrene Systems[a]

T/K	linear PS	WLF, $c_1 = 13.8$, $c_2 = 48$	log a_T, type A μgels	S10/10	S10/10F2
383	4.41	4.66			
393	2.83	2.99	3.04	3.96	
403	1.64	1.74	1.78	1.84	
413	0.73	0.77	0.79		1.56
423	0	0	0	0	0
433	−0.53	−0.63			
443	−1.05	−1.14	−1.19	−1.41	−2.00
453	−1.53	−1.59			
463	−1.85	−1.96	−2.31	−2.48	−3.34
473	−2.19	−2.28			
483	−2.45	−2.56		−4.32	

[a] The reference temperature was chosen as $T_{ref} = 423$ K.

Conversely, Adam et al. have determined a strictly scalable behavior as well that obeys the power law $G' \sim G'' \sim \omega^{0.7}$.[41] This scaling is in good agreement with data of Martin et al.[42,57] and Rubinstein et al.[43] In addition, Havranec et al. found a $J' \sim J'' \sim \omega^{-0.37}$ scaling for the sol fraction of near-critical gels.[44] These data agree with the frequency dependence of model micronetworks, where we observed scaling exponents α ranging between 0.20 and 0.55, depending on cross-linking density.[45] In this work, we detected an additional influence of entanglements with a scalable lifetime distribution, which causes deviation of the scaling exponents toward smaller values.

Winter also remarked that the ratio of G'' to G' must follow the Kramers–Kronig relation, which results in (taken from ref 46):

$$\arctan \frac{G''}{G'} = \frac{2\alpha}{\pi} \tag{12}$$

This relation is approximately fulfilled by all experiments listed above. Since we are interested in observing the frequency dependence in a range with maximal extension, we have to use the frequency/temperature superposition principle.[47] The master curves presented below are constructed by using only horizontal shifts. The resulting shift parameters, calculated for a reference temperature of 423 K, are listed in Table III. For comparison, additional data that have been determined by our group on linear polystyrenes are given. These values agree with literature values using the WLF parameters $c_1 = 13.8$ and $c_2 = 48$.[48]

The same data are graphically presented in Figure 6. For simplicity, the reference temperature for this presentation (where a_T is set to be zero) was chosen as $T_{ref} = T_g + 47$ K. The calorimetric glass transition T_g was determined by DSC as $T_g = 376$ K for linear polystyrene and $T_g = 391$ K for DVB microgels of the series S10/10.

The temperature dependence of the viscoelastic properties of the unfractionated sample S10/10 in between the glass transition and the reference temperature is very similar to that of linear polystyrene. At higher temperatures, the flattening of the curve is less pronounced, thus resulting in higher apparent activation energies.

This behavior is known from the temperature dependence of the diffusion coefficients of linear probe molecules in highly cross-linked polystyrene networks.[49,50] A possible description of such a behavior can be achieved with the coupling model of Ngai.[51] Within this model, a higher apparent activation energy in relation to linear chains corresponds to a large size of the cooperative domains due to cross-linking. A numerical fit of the temperature dependence with the WLF equation results, for the unfractionated sample, in parameters of $c_1 = 11.3$ and $c_2 = 47$.

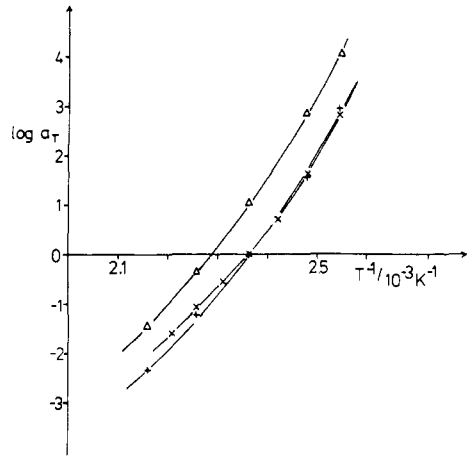

Figure 6. Shift parameter log a_T as obtained from dynamic mechanical shear experiments: (×) linear polystyrene; (+) cross-linked spherical microgels; (Δ) DVB microgels. The reference temperatures have been chosen as $T_{ref} = T_g + 47$ K.

It must be stated these WLF parameters, contrary to the corresponding ones of linear polymers, depend on the molecular weight of the fractions. For instance, the temperature dependence of the sample S10/10F2 is described by $c_1 = 17.2$ and $c_2 = 47$,[52] values that significantly deviate from those of the unfractionated sample. This unconventional coupling of size and temperature dependence will be subject of a forthcoming publication where the temperature dependence of transport properties in diverse microgels close to the glass transition will be discussed more extensively.[53]

The mechanical master curves for the storage modulus G', the loss modulus G'', and the dynamic viscosity η^* resulting from the temperature–frequency superposion for the unfractionated sample are presented in Figure 7.

We observe a strictly linear behavior of G', G'', and η^* over the whole accessible frequency range (more than seven decades). The scaling is limited only by the glass transition on the high-frequency side. At low frequencies, a further extension of the spectra is prohibited by the thermal stability of the samples. The slope of the G' and G'' curves is given by $\alpha = 0.72 \pm 0.03$.

In the present experiment, tan δ calculated from the slope (tan $\delta \approx 2.13$ via eq 11 is very close to the experimentally determined value (tan $\delta \approx 2.8$). This proves the absence of pronounced mechanisms of energy dissipation on the high-frequency side, e.g., the influence of very small polymer chains that contribute to the sample as demonstrated by the GPC spectra.

It must also be mentioned that the corresponding spectrum of the high molecular weight fraction, S10/10F2, is similar to that of the unfractionated sample: the slope and the loss angle are the same. Just the absolute values of G' and G'' are higher in case of the high molecular weight sample, which can be attributed to a higher monomer friction coefficient ζ_0 or a higher cooperativity of such a polymer melt.

Therefore, the absolute height of the spectrum corresponds to the anomalous behavior seen in the temperature dependence. The resulting master curves cannot be compared directly, and all differences should be attributed to the phenomenon of glass transition. Consequently, we restrict the discussion to the structural information that is included in the frequency dependence. In addition, we have to check whether the frequency scaling of the moduli is only due to intramolecular relaxation or whether it is influenced by intermolecular disturbances. For that, S10/10F2 has been diluted with 70%, 50%, and 30% of linear chains ($M_w \approx 102\,000$ g/mol, $M_w/M_n < 1.03$). In these cases, no changes in the slope have been observed, whereas the absolute heights of the spectra strongly decrease and tan δ slightly changes toward smaller values. This demonstrates that the observed dynamic behavior is strictly intramolecular.

III.5. Relation to Other Experiments and Comparison with Theory. It is worth mentioning that the critical DVB microgels, although their critical nature is obtained by dilution during cross-linking, obey the same dynamics as the critical structures of Durand et al.,[41] Martin et al.,[42] Rubinstein et al.,[43] and Adolf and Martin.[57] The latter four systems only become critical by stopping the reaction at the critical conversion of the reaction. Especially, we must refer to the work of Adolf and Martin,[57] who used a "time-cure-superposition-principle" and have determined exactly the same exponent ($\alpha = 0.72$) holding over a similar span of frequencies.

In contrast to this class of systems, polystyrene micronetworks synthesized by end-linking reactions behave differently. They obey scaling rules with exponents between 0.2 and 0.5, where the exponent depends on the cross-link density. In addition, their dynamic response can be separated into an intramolecular relaxation with a $\omega^{0.5}$ dependence and a contribution by intermolecular entanglements. We believe that these results can be related to the experiments of Winter et al.[39,41] Here, unfractionated samples are examined, and the behavior of critical clusters in dilution is observed. Obviously, the critical neighborhood to the gel transition determines only a scaling but not the exponent of the scaling laws. It looks like further criteria for diversification are necessary. This point will be discussed below.

Since we have determined not only the scaling exponent of the radial density function (d_f, spatial dimension of the system) but also that of the dynamic spectrum of the same systems, it is straightforward to relate these quantities via the theory of fractals.

This relation was first formulated by Muthukumar[54] and results in

$$G' \sim G'' \sim \omega^{\alpha} \qquad \alpha = 1 - \frac{2}{2 + d_f} \tag{13}$$

This formula was successfully applied to the Winter systems[40] under the assumption that the critical network underlies excluded volume effects.

It is evident that this simple prediction does not describe our data; e.g., the calculated α value ($\alpha \approx 0.51$) clearly deviates from the measured value ($\alpha \approx 0.72$).

More complex models like those of Daoud[55] or Rubinstein et al.,[43] which correct the dynamic spectrum for excluded volume effects, result in exponents of $\alpha \approx 0.67$, a value in the magnitude range of the experimental data. However, we have clearly proven that DVB microgels are too stiff to show excluded volume effects (by the similarity of d_f determined with SANS and light scattering). The agreement between theory and experiment may therefore occur accidentally. In addition, it is not evident why these descriptions fail in case of the Winter experiments or in describing the behavior of the end-linked micronetworks.

For an explanation of these differences and the necessity of further classification, we follow the opinion of Martin et al.[42] who have speculated that the deviations are caused by the difference in chemistry. It is uncertain if the static percolation model can be realized with a chemical system, since existing cross-links modify the reactivity or the cross-linking topology of their neighbors (see, for instance, ref 27). Also, end-linking reactions and vulcanizations should

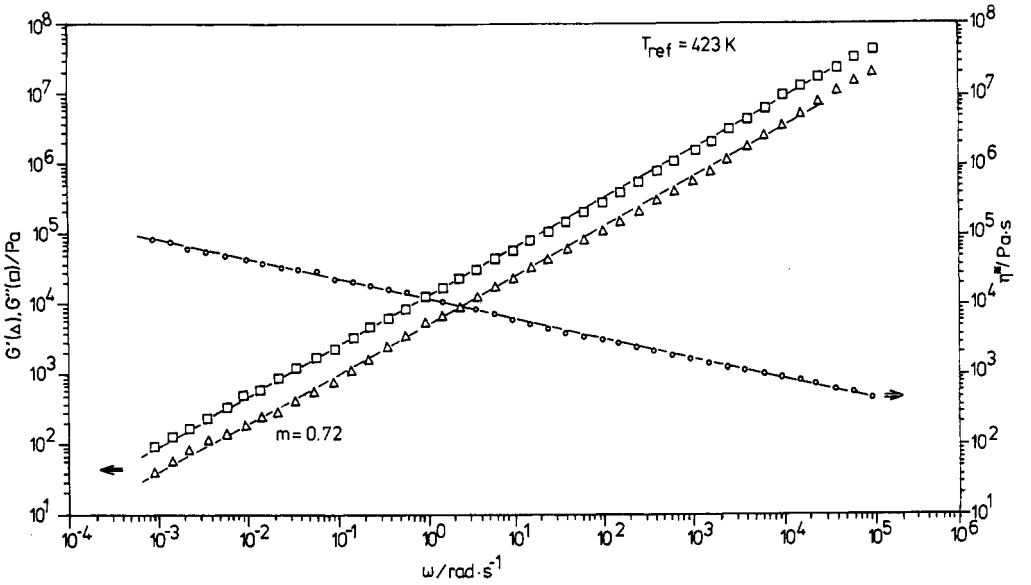

Figure 7. Master curves of the dynamic mechanical behavior of S10/10: storage modulus G' (Δ), loss modulus G'' (□), and dynamic shear viscosity η^* (○) versus the shear frequency ω. The temperature/frequency superposition principle has been applied where the reference temperature has been chosen as T_{ref} = 423 K.

result in different products, since their topology of cross-linking and the tendency toward side reactions differ a lot.

We have already proposed that the inner structure of DVB microgels is better described by a dynamic aggregation model (dynamic percolation, DP) than by static percolation (SP). In contrast to SP, the mechanism and kinetics of bond formation play an important role in DP models, where spatial dimensionalities with exponents between $d_f \approx 1.8$ (diffusion limited cluster/cluster aggregation) and $d_f = 3$ (reaction limited monomer/cluster aggregation) are obtained. From a chemical point of view, this reflects the spectrum of potential microgel structures better.

The disadvantage of all kinetic aggregation models is that a transition from macro- to microgelation is not predicted in an obvious way, at least not at the present state of the simulations.

We can speculate that the appropriate description of the gel transition contains indeed some components of the SP description. However, the influennce of dynamic processes during addition of the elementary units on a local scale, as delineated in the DP models, must also be considered. To our knowledge, this is not performed in existing theoretical treatments. It is not surprising that simple SP predictions partly fail in case of "real" gelling systems.

IV. Summary and Conclusion

In this work, we have repeated the Staudinger/Husemann experiments for the controlled synthesis of microgels first performed in 1935. As these systems were synthesized just below the transition from micro- to macrogelation, they exhibit a scalable behavior of their static and dynamic properties and can be described as fractals. The spatial dimensionality of these systems is given by $d_f = 2.15 \pm 0.05$. Since the d_f values determined by light and neutron scattering coincide, the scaling relationship of the inner density is fulfilled on a length scale spanning more than 2 orders of magnitude in size. The uncertainty of d_f mainly results from the fact that we had to fractionate the sample to allow the determination of molecular weight dependencies. This procedure is generally disturbed by a secondary polydispersity that describes the distribution

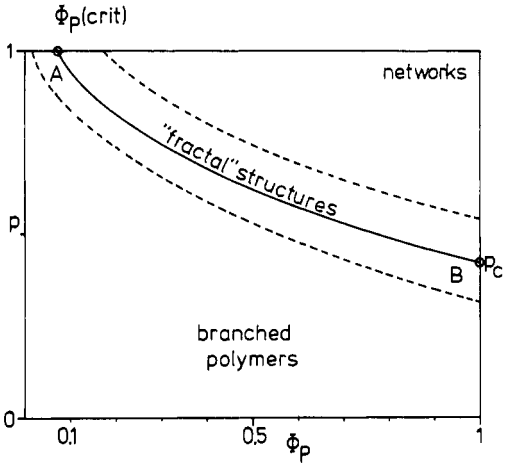

Figure 8. Phase diagram for cross-linking reactions. The solid line represents the curve of the sol–gel transition versus the extent of reaction, p, and the volume fraction of polymer during cross-linking, Φ_P. Close to the gel curve, structures with fractal properties are formed. This regime is estimated to be between the dotted lines. Within this regime, the fractal character decreases with increasing distance from the gel curve. A and B represent the regions where referred systems have been synthesized.

of the molecular hydrodynamic volumes at a given molecular weight.

Figure 8 presents a schematic "phase diagram" for cross-linking reactions. Here, the formation of different structures is plotted versus the extent of reaction, p, and the volume fraction of polymer during cross-linking, Φ_P. Due to the increasing amount of inner cyclization, the classical gel point (at $\Phi_P = 1$) is only the starting point for a gel curve. This curve also has an intercept at $p = 1$, which means that below a critical volume fraction Φ_P(crit) no macroscopic gelation occurs and microgels are formed.

The Staudinger microgels synthesized in this region (domain A) exhibit static and dynamic properties similar to the critical systems that are made by stopping the reaction at a critical conversion (domain B). A comparison with model micronetworks (ref 7, also synthesized in domain A) and with copolymers made of styrene and divinyltetrachlorobenzene[30] shows that the molecular weight dependences of the size and inner density are very similar

and independent of the cross-linking density. This indicates some universality of the architecture of microgels synthesized just below the gel curve, although pronounced differences in the local structure exist, as shown by SANS. This similarity is a strong indication that the classical gel point can be generalized by inclusion of all effects of dilution, most importantly the inner cyclization.

With dynamic mechanical shear experiments, we observe also a scalable behavior of dynamic properties of DVB microgels. Here, the exponent of the frequency dependence of G' and G'' is given by $\alpha = 0.72 \pm 0.03$, a value that agrees well with reported literature values.

However, a quantitative interrelation between the scaling exponents of the static structure and the dynamic relaxation fails, indicating a more complex structure than would be predicted by static percolation theory.

Since the Staudinger microgels are synthesized in dilution, one can assume that the local structure is better described by dynamic aggregation models (dynamic percolation), although these models do not describe a transition between micro- and macrogelation. It must be pointed out that every critical system described in the literature is synthesized in domain B, where static percolation may be more appropriate for the description of gelation. However, we cannot use this argument as a criterium for separation or classification since the transition from A to B systems will occur continuously. Even a cross-linking reaction performed in the bulk will be influenced by excluded volume effects, which is one experimental consequence of the nonideality of cross-linking in 3d space.[56] This confirms our position that a correct theoretical description of critical polymer gels must consist of elements of static and dynamic percolation.

Acknowledgment. We especially thank M. Schmidt, H. Sillescu, and T. Vilgis for many helpful comments and discussions. We are also indebted to T. Pakula for his competent help with mechanical experiments and to P. Lindner for his aid during the SANS part of this work. Financial support by the Deutsche Forschungsgemeinschaft is gratefully acknowledged.

References and Notes

(1) Staudinger, H.; Husemann, E. *Ber.* **1935**, *68*, 1618.
(2) Funke, W. E. *J. Coat. Technol.* **1988**, *60*, 69.
(3) Ishikura, S.; Ishii, K.; Midzuguchi, R. *Prog. Org. Coat.* **1988**, *15*, 373.
(4) Seitz, U.; Pauly, H. E. *Angew. Makromol. Chem.* **1979**, *76*, 316.
(5) Funke, W. *Br. Polym. J.* **1989**, *21*, 107.
(6) Antonietti, M. *Angew. Chem.* **1988**, *100*, 1813.
(7) Antonietti, M.; Ehlich, D.; Fölsch, K. J.; Sillescu, H.; Schmidt, M.; Lindner, P. *Macromolecules* **1989**, *22*, 2802.
(8) Antonietti, M.; Bremser, W.; Fölsch, K. J.; Sillescu, H. *Makromol. Chem. Macromol. Symp.* **1989**, *33*, 81.
(9) Höcker, H.; Reif, L. *Makromol. Chem. Rapid Commun.* **1981**, *2*, 745.
(10) Bantle, S.; Schmidt, M.; Burchard, W. *Macromolecules* **1982**, *15*, 1604.
(11) Antonietti, M.; Sillescu, H.; Schmidt, M.; Schuch, H. *Macromolecules* **1988**, *21*, 736.
(12) Neutron Research Facilities at the ILL High Flux Reactor, ILL, Grenoble, June 1986.
(13) Flory, P. J. *J. Am. Chem. Soc.* **1941**, *63*, 3083, 3091, 3096.
(14) Stockmayer, W. H. *J. Chem. Phys.* **1943**, *11*, 45.
(15) Flory, J. P. *Principles of Polymer Chemistry*; Cornell University Press: Ithaca, NY, 1953.
(16) Schosseler, F.; Benoit, H.; Gallot, Z.; Strazielle, C.; Leibler, L. *Macromolecules* **1989**, *22*, 400.
(17) Schmidt, M.; Burchard, W. *Macromolecules* **1981**, *14*, 370.
(18) Malinski, J.; Klabau, J.; Dusek, K. *J. Makromol. Sci.* **1971**, *A5*, 1071.
(19) Soper, B.; Harvard, R. N.; White, E. F. T. *J. Polym. Sci. A1* **1972**, *10*, 2545.
(20) Dusek, K.; Galiva, H.; Mikes, H. *Polym. Bull.* **1980**, *3*, 19.
(21) Dusek, K. *Makromol. Chem. Suppl.* **1979**, *2*, 35.
(22) Seitz, U. *Makromol. Chem.* **1977**, *178*, 1689.
(23) Yamakawa, H. *Modern Theory of Polymer Solutions*; Harper & Row: New York, 1971.
(24) Roovers, J.; Toporowski, M. *J. Polym. Sci., Polym. Phys. Ed.* **1980**, *18*, 1907.
(25) Schmidt, M.; Burchard, W. *Macromolecules* **1981**, *14*, 210.
(26) Schmidt, M.; Nerger, D.; Burchard, W. *Polymer* **1979**, *20*, 582.
(27) Antonietti, M.; Bremser, W.; Schmit, M. *Macromolecules* **1990**, *23*, 3796.
(28) Grubisic, Z.; Rempp, P.; Benoit, H. *J. Polym. Sci., Polym. Lett. Ed.* **1967**, *5*, 753.
(29) Kurata, M.; Abe, M.; Iwana, M.; Matsushima, M. *Polym. J.* **1972**, *3*, 729.
(30) Feigin, L. A.; Svergun, D. I. *Structure Analysis by Small Angle X-Ray and Neutron-Scattering*; Plenum Press: New York, 1987.
(31) de Gennes, P.-G. *Scaling Concepts in Polymer Science*; Cornell University Press: Ithaca, NY, 1979.
(32) Teixera, J. *J. Appl. Crystallogr.* **1988**, *21*, 781.
(33) Schaefer, D. *Science* **1989**, *243*, 1023.
(34) Chu, B.; Wu, C.; Wu, D.; Phillips, J. C. *Macromolecules* **1987**, *20*, 2643.
(35) Bouchaud, E.; Delsanti, M.; Adam, M.; Dauod, M.; Durand, D. *J. Phys.* **1986**, *47*, 1273.
(36) Stauffer, D.; Coniglio, A.; Adam, M. *Adv. Polym. Sci.* **1982**, *44*, 103.
(37) Vilgis, T. *Makromol. Chem., Rapid. Commun.* **1988**, *9*, 513.
(38) Chambon, F.; Winter, H. H. *J. Rheol.* **1986**, *30/2*, 367.
(39) Muthukamar, M.; Winter, H. H. *Macromolecules* **1986**, *19*, 1284.
(40) Chambon, F.; Pertrovic, Z. S.; MacKnight, W. J.; Winter, H. H. *Macromolecules* **1986**, *19*, 2146.
(41) Durand, D.; Delsanti, M.; Adam, M.; Luck, J. M. *Europhys. Lett.* **1987**, *3*, 297.
(42) Martin, J. E.; Adolf, D.; Wilcoxon, J. P. *Phys. Rev. Lett.* **1988**, *61*, 2620.
(43) Rubinstein, M.; Colby, R. H.; Gillmor, J. R. *Polym. Prepr.* **1989**, *30*, 81.
(44) Havranec, A.; Ilavski, M.; Nedbal, J.; Böhm, M.; v. Soden, W.; Stoll, B. *Colloid Polym. Sci.* **1987**, *265*, 8.
(45) Antonietti, M.; Fölsch, K. J.; Sillescu, H.; Pakula, T. *Macromolecules* **1989**, *22*, 2812.
(46) teNijenhuis, K.; Winter, H. H. *Macromolecules* **1989**, *22*, 411.
(47) Ferry, J. D. *Viscoelastic Properties of Polymers*, 3rd ed.; Wiley: New York, 1980.
(48) Allen, G.; Fox, T. G. *J. Chem. Phys.* **1979**, *41*, 337.
(49) Antonietti, M.; Sillescu, H. *Macromolecules* **1985**, *18*, 1162.
(50) Fölsch, K. J. Dissertation, Mainz, 1988.
(51) Ngai, K. L.; Mashimoto, S.; Fytas, G. *Macromolecules* **1988**, *21*, 3030.
(52) Antonietti, M. Habilitation, Mainz, 1990.
(53) Antonietti, M.; Sillescu, H., unpublished results.
(54) Muthukumar, M. *J. Chem. Phys.* **1985**, *83*, 3161.
(55) Daoud, M. *J. Phys.* **1988**, *A21*, L237.
(56) Vilgis, T. A. *Phys. Rev. A* **1987**, *36*, 1506.
(57) Adolf, D.; Martin, J. E. *Macromolecules* **1990**, *23*, 3700.

Registry No. (St)(DVB) (copolymer), 9003-70-7.